Journal of Alloys and Compounds 446–447 (2007) 562–566

Journal of ALLOYS AND COMPOUNDS

www.elsevier.com/locate/jallcom

New insights from Raman and IR spectroscopy into the metal-insulator transition of YH_x switchable mirrors

J. Schoenes*, A.-M. Racu, M. Rode, S. Weber

Institut für Physik der Kondensierten Materie, Technische Universität Braunschweig, Mendelssohnstrasse 3, D-38102 Braunschweig, Germany

Received 20 September 2006; received in revised form 21 December 2006; accepted 24 December 2006

Abstract

The important recent contributions of elastic and inelastic light scattering to our understanding of the electronic structure and the metal-insulator transition of the switchable-mirror prototype material YH_x will be reviewed. In particular, we will discuss the striking broadening with increasing temperature of one single Raman line, corresponding to a breathing mode of Y atoms surrounding a hydrogen site. It is shown that the extra broadening is due to electron–phonon coupling and that it follows an Arrhenius law with an activation energy of 0.09 eV. A close inspection of our IR spectra shows at the same energy an absorption line with an anomalous temperature dependence, which results from the overlap of a phonon and an electron excitation. This energy is assigned to the activation of electrons trapped in hydrogen vacancies, corroborating the correlated electron models for the electronic structure.

Keywords: Thin films; Vapor deposition; Electron–phonon interactions; Electronic band structure; Optical spectroscopy

1. Introduction

Although metal hydrides are known since 1866 when Graham [1] reported that Pd can absorb a large quantity of hydrogen, the mechanism of this take up, i.e. the involved metal-insulator transition is still debated. A major reason is that before switchable mirrors had been discovered in 1996 [2], powerful techniques to study the electronic structures of solids, like optical and photoelectron spectroscopies, could not be applied effectively. Since then, a growing number of experiments [3–8] points to a correlated description of the electronic structure of the prototype YH_x system, in agreement with some of the theoretical models put forward recently for YH_x or LaH_x [9,10]. This contradicts earlier attempts to describe these materials with simple one-electron band structure calculations [11–13] and conflicts with the idea that hydrogen enters into the metal lattice as proton. Strongly correlated electron models have been applied successfully in the last decades to describe heavy Fermion systems and high-temperature superconductors, but the appeal of these models may also have lead in some cases to a premature label [14,15]. In this paper, we will review recent Raman [6] data and present additional new IR and Raman data which give further evidence for the strongly correlated electron behavior of switchable mirrors.

2. Experimental details

Yttrium films have been grown by molecular beam epitaxy in a vacuum better than 1×10^{-9} mbar by electron-gun evaporation. The substrates for all Raman and some IR experiments were (1 0 0)-oriented “epi-ready” commercial CaF_2 crystal plates which were cleaned by heating to 700 °C [16]. The optimum deposition temperature is also 700 °C. Since CaF_2 absorbs light for wave numbers below 300 cm^{-1}, some transmission measurements in this spectral range have been performed on polycrystalline films grown on Si wafers. To protect the films against oxidation and to dissociate the molecular hydrogen, the films were covered with 10 nm thick Pd layers. The samples were then loaded in a gas cell with H_2 or D_2 at a pressure of 1 bar.

Raman spectra have been recorded, using a commercial micro-Raman spectrometer (Jobin Yvon LabRam HR). The excitation radiation is the 532 nm wavelength line of a diode-pumped Nd:YAG (yttrium aluminium garnet) laser of 150 mW. The light beam is focused on an area of a few μm^2, depending on the magnification of the microscope objective. The Raman measurements are performed through the transparent substrate side.

The IR reflectivity and absorption spectra were recorded with a commercial Fourier transform spectrometer (Bruker FT-IR 113v). To cover the full spectral range of the spectrometer, three radiation sources can be used. For the near IR a halogen lamp is available. The mid-IR is covered with a globar and the far IR

---

* Corresponding author. Tel.: +49 531 391 5130; fax: +49 531 391 5155.
E-mail address: j.schoenes@tu-bs.de (J. Schoenes).

0925-8388/$ – see front matter © 2007 Elsevier B.V. All rights reserved.
doi:10.1016/j.jallcom.2006.12.141

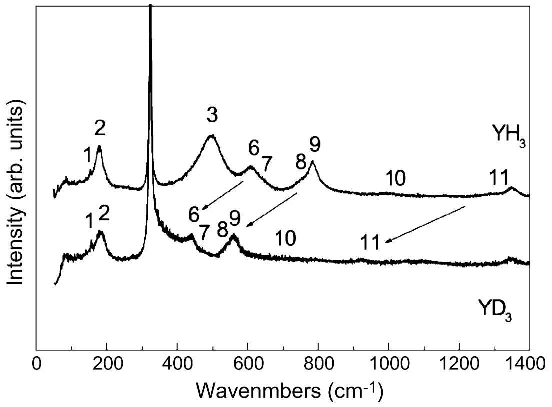

Fig. 1. Room temperature micro-Raman spectra for YH_3 and DH_3. The arrows indicate the frequency shifts of the hydrogen vibrations.

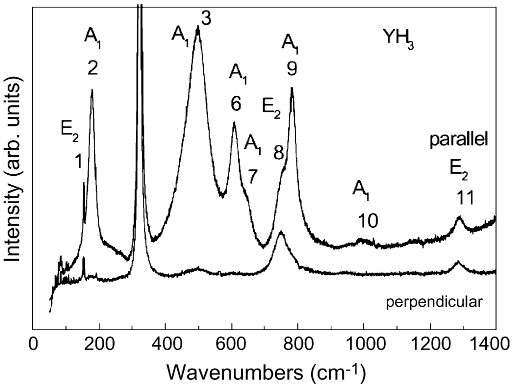

Fig. 2. The effect of polarization on the room-temperature micro-Raman spectra of YH_3. A_1 modes appear only for parallel polarization, while E_2 modes show up for both polarizations.

makes use of a mercury-discharge lamp. The radiation detectors include, from the near to the far infrared range, InSb, HgCdTe and deuterated triglicin sulfate (DTGS) detectors and a Si bolometer. The radiation is focused onto an area of a few mm^2. Both spectrometers are equipped with a helium cryostat, allowing measurements down to approximately 4 K, the lowest achievable temperature depending on the intensity of the illumination. For Raman measurements above 300 K an oven has been constructed, allowing measurements up to 450 K.

3. Results and discussion

The first Raman spectra for YH_x with $x \cong 2$ and 3 have been obtained by Kierey et al. with a home built "macro-Raman spectrometer" [4]. Although all lines could be observed, the spectra suffered from an overlap with broader structures originating from the CaF_2 substrate. Defects of fluorine introduced by the heating of the substrate for cleaning and optimal growth purposes give rise to otherwise forbidden Raman excitations. Fig. 1 displays Raman spectra for $YH_{3-\delta}$ and $YD_{3-\delta}$ films recorded with the micro-Raman spectrometer at room temperature. Except for the intrinsic Raman active mode of CaF_2 at 322 cm^{-1}, no other CaF_2 mode is visible, although these measurements have been performed like the macro-Raman measurements through the CaF_2 substrate. The reason is the strong focusing of the light beam on the $YH_{3-\delta}$ film and the confocal imaging which reduces the amount of scattered light from the CaF_2 substrate falling into the monochromator. The comparison of the $YH_{3-\delta}$ and $YD_{3-\delta}$ spectra shows clearly that the high frequency modes 3–11 correspond to H or D vibrations, respectively, while the low frequency modes 1 and 2 involve Y vibrations. In $YD_{3-\delta}$ the line 3 is hidden under the strong CaF_2 line. It appears as small shoulder on the high energy side of the CaF_2 line from the substrate. Also in $YH_{3-\delta}$ at low temperatures two more lines appear near 500 cm^{-1} [6], explaining the missing of line labels 4 and 5 in Fig. 1. The symmetry of the observed Raman lines has been tested by comparing polarization resolved spectra [4]. Fig. 2 shows the analogous micro-Raman spectra at room temperature. Modes with A_1 symmetry appear only for parallel polarization, while E_2 modes show up for parallel and perpendicular polarization. From a systematic analysis of such polarization dependent Raman spectra and spectra taken at different angles of incidence, Kierey et al. [4] concluded that the crystal structure of $YH_{3-\delta}$ is noncentrosymmetric, which excludes the earlier proposed centrosymmetric $P\bar{3}c1$ structure [17] and promotes the $P6_3cm$ structure. We like to concentrate now on the Y vibrations. Fig. 2 shows clearly that lines 1 and 2 have different symmetries. Line 2 with A_1 symmetry corresponds to a breathing mode of six Y atoms surrounding a hydrogen atom on an octahedral site (Fig. 3a). In contrast, line 1 with symmetry E_2 corresponds to a scissor oscillation of two pairs of opposite yttrium atoms (Fig. 3b).

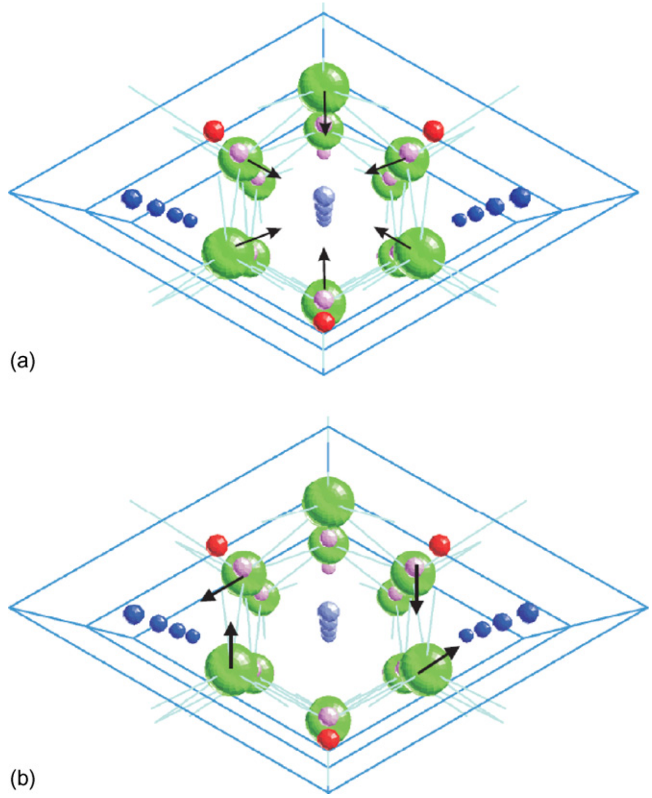

Fig. 3. A_1 breathing (a) and E_2 scissor-oscillator mode (b) of YH_3 in the $P6_3cm$ space group. The big (green) circles represent the yttrium atoms. The (light blue, dark blue, red and pink) small circles are the hydrogen atoms on octahedral (light and dark blue) and tetrahedral (red and pink) sites. The arrows show the displacement of the yttrium atoms around an octahedral hydrogen site. (For interpretation of the references to color in this figure legend, the reader is referred to the web version of the article.)

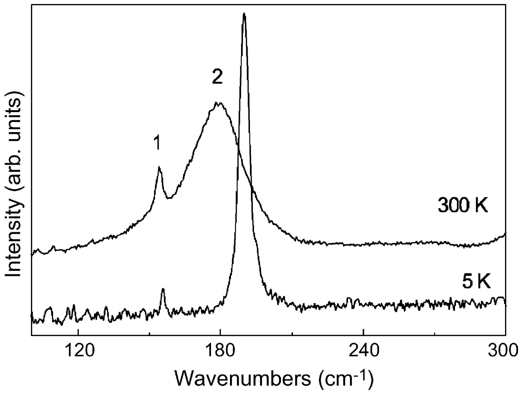

Fig. 4. Raman spectra of YH_3 for parallel polarization in the frequency range of the yttrium vibrations at 5 and 300 K.

Fig. 4 displays enlarged parts of the Raman spectra for the Y vibrations in $YH_{3-\delta}$ at 5 and 300 K. One clearly sees an anomalous line broadening of line 2 with increasing temperature. This broadening is not only one order of magnitude larger than that of line 1, but it is also much larger than the broadening of all hydrogen lines. To assess this quantitatively, the line shapes of the $YH_{3-\delta}$ peaks have been fitted with Lorentzian functions with full width at half maximum (FWHM) Γ. Fig. 5 displays the temperature dependence of Γ normalized with the respective phonon frequency ω_0 for the two yttrium vibrations 1 and 2 and line 9 as a typical example for the hydrogen vibrations. While the temperature range for these measurement was previously limited on the high temperature side by the cryostat to 320 K [6], we have now constructed an oven allowing to extend the micro-Raman measurements up to 450 K. With this innovation, one clearly sees that the strong increase of Γ/ω_0 saturates for line 2 around 400 K, while the weak increase of Γ/ω_0 for lines 1 and 9 persists for all temperatures.

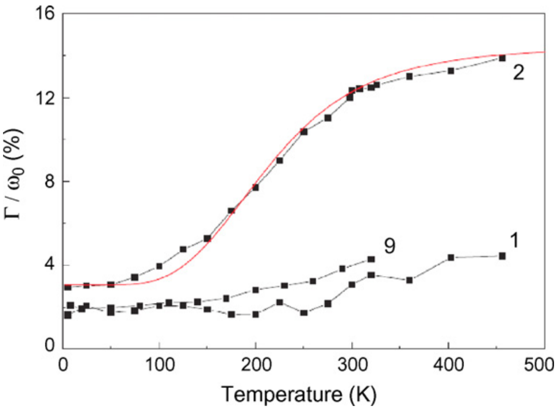

Fig. 5. Temperature dependence of the normalized width for the two yttrium (1 and 2) and one hydrogen (9) vibration modes in $YH_{3-\delta}$. The solid line is a fit using Eqs. (1) and (2).

The most common process governing linewidths of excited optical phonons is the decay into two longitudinal acoustic modes [18]. This process leads to rather weak line broadenings, as exemplified by the behavior of lines 1 and 9 in Fig. 5. Another channel for the decay of phonons comes from electron–phonon coupling. As was shown by Axe and Shirane [19] in inelastic neutron scattering experiments for the superconductor Nb_3Sn and by Nyhus et al. [20] in Raman experiments on the small gap semiconductor FeSi, the normalized electron–phonon linewidth contribution can be expressed as

$$\frac{\Gamma}{\omega_0} = \pi N(0)\hbar\omega_0\lambda, \tag{1}$$

where $N(0)$ is the density of states at the Fermi surface and λ is the electron–phonon coupling parameter due to the considered phonon. While in the superconductor the phonon damping involves resonant scattering with electrons created by Cooper-pair breaking, in the small gap semiconductor the free electrons are generated by excitation of electrons from the valence into the conduction band. In our case, the temperature dependence of the linewidth shown in Fig. 5 suggest that the electrons are excited from a donor level and we fit the experimental data with an expression for a doped semiconductor, giving the number of free carriers $N(T)$ as function of the donor concentration N_D and the activation energy E_d as [21]:

$$N(T) = \frac{2N_D}{1+\sqrt{1+4(N_D/N_C)\exp(E_d/kT)}}. \tag{2}$$

Here N_C is the density of states in the conduction band, which depends on the temperature as $T^{3/2}$. The full line in Fig. 5 shows the fit of the normalized linewidth of line 2 with Eqs. (1) and (2). Note in particular, the good fit also at high temperature when the donor state is exhausted and, therefore, the free carrier concentration remains constant. The remaining weak increase of Γ/ω_0 reflects the phonon–phonon interaction which has not been subtracted, since its contribution is small compared to the electron–phonon contribution and its consideration would have increased the number of fit parameters. Instead, the only relevant parameter of our fit is the activation energy E_d of 0.09 eV. This value is somewhat smaller than the rough estimate of Ng et al. [10] of 0.38 eV for $LaH_{3-\delta}$, but considering the crudeness of this estimation and the fact that we are dealing with $YH_{3-\delta}$ and not $LaH_{3-\delta}$, makes us confident that this donor level corresponds to the hydrogen vacancy state on an octahedral site, as postulated in the strongly correlated electron model of Ng et al. [10].

Before we discuss this model in more detail, we present additional evidence for the existence of the donor state. Indeed, if the octahedral site of the hydrogen vacancy captures an electron which forms a donor state with an activation energy $E_d = 0.09\ \text{eV} \cong 726\ \text{cm}^{-1}$, one ought to see in IR spectroscopy an absorption at the corresponding frequency. Fig. 6 displays reflectivity spectra in the IR for various temperatures from 20 to 280 K. One sees four lines which have been assigned previously to the excitation of phonons [5]. However, the present systematic study reveals that the line near 730 cm^{-1} shows a markedly different intensity behavior than the three other lines, pointing to a different origin, although Raman measurements under an angle of incidence of 45° indicate at this energy the existence of an E_1 phonon [4] which should also be IR active. Fig. 7 helps to resolve the problem. It shows the normalized oscillator strength of the line at 727 cm^{-1}, and for comparison also for two other lines from a fit with Lorentz oscillators of the spectra in Fig. 6. One notes, the strong decrease of the intensity with

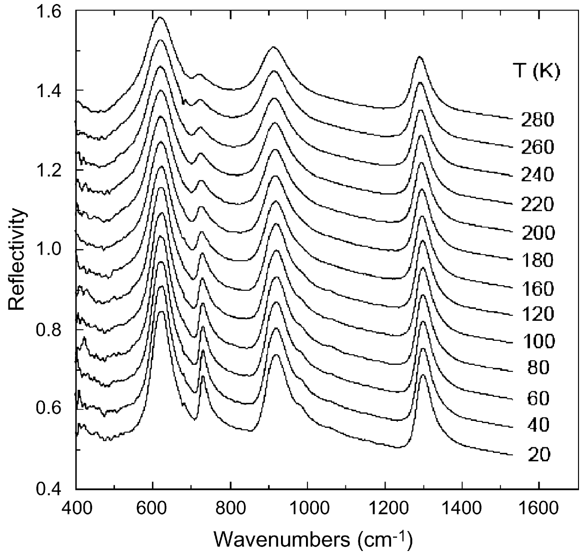

Fig. 6. Infrared reflectivity spectra of $YH_{3-\delta}$ for various temperatures between 20 and 280 K. For clarity consecutive spectra are shifted by a constant value.

increasing temperature for the former line and the tendency for saturation near room temperature, while for the two latter a much weaker decrease of the normalized intensity appears to persist even beyond room temperature. We conclude that one is dealing near 730 cm^{-1} with the overlap of a phonon which is responsible for about 30% of the intensity at the lowest temperatures and an electronic transition whose contribution decreases from about 70% at low temperatures to ≅0% near 300 K. Similarly to the situation of the broadening of the Raman line, the intensity of the electronic transition has to vanish when all donors have been excited thermally. Thus, the IR measurements beautifully corroborate the existence of a donor level about 0.1 eV below the conduction band edge.

Such a donor level has been anticipated in the model of the electronic structure of Ng et al. for $LaH_{3-\delta}$ [10]. In their model LaH_3 is viewed as a Kondo insulator with a large band gap. Starting from the metallic LaH_2, every additional H atom is considered as a Kondo impurity. The hydrogen atoms attract one more electron and form H^- ions. The correlation between the two electrons then leads to a bound H^- state, very much like the Zhang–Rice singlet formed by holes in the high temperature superconductors [22]. The strong electron correlations suppress the overlap between the hydrogen and the lanthanum bands, leading to the gap formation when the ratio of hydrogen to lanthanum comes close to three. On the other hand, if one starts from stoichiometric LaH_3, every missing hydrogen atom will capture an electron forming a localized electronic state on the vacancy. The transition to the metallic state occurs when these localized states overlap sufficiently to form a band.

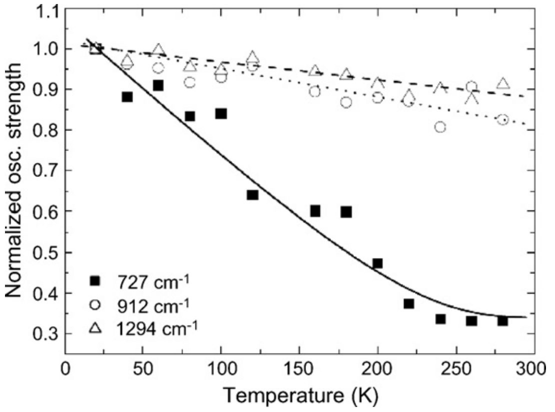

Fig. 7. Temperature dependence of the oscillator strength normalized to its value at 20 K for three reflectivity maxima of Fig. 7. The lines are guides to the eye.

Optical spectroscopy has provided large evidence for the above model. In a first paper [3], we have shown by an analysis of the dielectric function in the infrared that YH_3 is a highly ionic compound with a charge transfer of ≅1.5e^- from each yttrium atom to hydrogen, giving an effective Szigeti charge of 0.5e^- on each hydrogen atom. In a second paper [4], the crystal structure of $YH_{3-\delta}$ was investigated by Raman spectroscopy, excluding some crystallographic structures which had been suggested to allow for a gap formation in LDA computations of the electronic structure. A further Raman study [6] which we have also discussed here, presented evidence for the coupling of a breathing-phonon mode with electronic d states of the Y conduction band. Finally, a systematic investigation of IR absorption (not shown) and reflectivity spectra proves the existence of the hydrogen vacancy related donor state with approximately 0.1 eV binding energy.

4. Conclusions

We have reviewed some of the recent Raman results evidencing electron–phonon coupling between a particular phonon mode and free carriers excited from a donor level. The existence of these donor levels is corroborated by new IR investigations. These and earlier results from IR and Raman spectroscopy are shown to support the description of switchable mirrors and, likely, also other insulating metal hydrides in terms of a strongly correlated electron model.

References

[1] T. Graham, Phil. Trans. Roy. Soc. London 156 (1866) 399.
[2] J.N. Huiberts, R. Griessen, J.H. Rector, R.J. Wijngaarden, J.P. Dekker, D.G. de Groot, N.J. Koeman, Nature (London) 380 (1996) 225.
[3] M. Rode, A. Borgschulte, A. Jacob, C. Stellmach, U. Barkow, J. Schoenes, Phys. Rev. Lett. 87 (2001) 235502.
[4] H. Kierey, M. Rode, A. Jacob, A. Borgschulte, J. Schoenes, Phys. Rev. B 87 (2001) 134109.
[5] J. Schoenes, A. Borgschulte, A.-M. Carsteanu, H. Kierey, M. Rode, J. Alloys Compd. 356–357 (2003) 211.
[6] A.-M. Racu, J. Schoenes, Phys. Rev. Lett. 96 (2006) 017401.
[7] J. Hayoz, C. Koitzsch, M. Bovet, D. Naumovic, L. Schlapbach, P. Aebi, Phys. Rev. Lett. 90 (2003) 196804.
[8] C. Koitzsch, J. Hayoz, M. Bovet, F. Clerc, L. Despont, C. Ambrosch-Draxl, P. Aebi, Phys. Rev. B 70 (2004) 165114.
[9] R. Eder, H.F. Pen, G.A. Sawatzky, Phys. Rev. B 56 (1997) 10115.
[10] K.K. Ng, F.C. Zhang, V.I. Anisimov, T.M. Rice, Phys. Rev. B 59 (1999) 5398.
[11] Y. Wang, M.Y. Chou, Phys. Rev. B 51 (1995) 7500.
[12] J.P. Dekker, J. van Ek, A. Lodder, J.N. Huiberts, J. Phys. Condens. Mat. 5 (1993) 4805.
[13] P.J. Kelly, J.P. Dekker, R. Stumpf, Phys. Rev. Lett. 78 (1997) 1315.

[14] J. Schoenes, R.L. Withers, F. Hulliger, Proc. Intern. Conf. Magnetism 2006, J. Magn. Magn. Mat., in press.

[15] D. Zur, D. Menzel, I. Jursic, J. Schoenes, L. Patthey, M. Neef, K. Doll, G. Zwicknagl, Phys. Rev. B., in press.

[16] A. Jacob, A. Borgschulte, J. Schoenes, Thin Solid Films 414 (2002) 39.

[17] T.J. Udovic, Q. Huang, J.J. Rush, J. Phys. Chem. Solids 57 (1995) 423.

[18] J. Jimenez, E. Martin, A. Torres, J.P. Landesman, Phys. Rev. B 58 (1998) 10463.

[19] J.D. Axe, G. Shirane, Phys. Rev. Lett. 30 (1973) 214.

[20] P. Nyhus, S.L. Cooper, Z. Fisk, Phys. Rev. B 51 (1995) 15626.

[21] H. Ibach, H. Lüth, Festkörperphysik, 4th ed., Springer Lehrbuch, New York, 1995.

[22] F.C. Zhang, T.M. Rice, Phys. Rev. B 37 (1988) 3759.